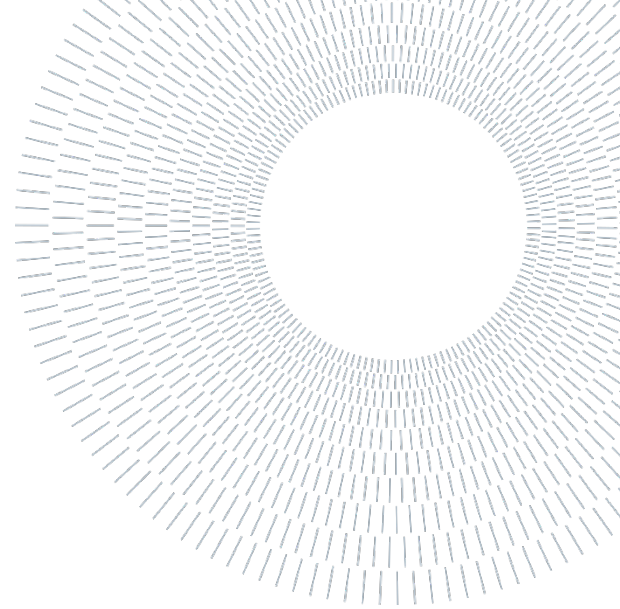




**POLITECNICO**  
MILANO 1863

SCUOLA DI INGEGNERIA INDUSTRIALE  
E DELL'INFORMAZIONE



EXECUTIVE SUMMARY OF THE THESIS

## MID-FIDELITY MODELING OF THE AERO-PROPULSIVE INTERACTION FOR THE INITIAL DESIGN OF DISTRIBUTED PROPULSION AIRCRAFT

TESI MAGISTRALE IN AERONAUTICAL ENGINEERING – INGEGNERIA AERONAUTICA

**AUTHOR: ANDREA ROBERTO MORETTI**

**ADVISOR: LORENZO TRAINELLI**

**ACADEMIC YEAR: 2021-2022**

### 1. Introduction

This thesis presents the development of a mid-fidelity meta-model for the aero-propulsive interaction of distributed propulsion aircraft, which is suitable for preliminary aircraft sizing. The meta-model represents a generic and comprehensive approach able to provide meaningful information concerning aero-propulsive effects in the early phase of the design process. It aims to increment the accuracy of existing sizing routines without compromising their rapidity.

#### 1.1. Distributed Electric Propulsion

Electric vehicles are a viable solution to reduce noise and air pollution in densely populated urban areas. However, the weight penalty associated with batteries still represents a significant limit to electric aircraft development. In this context, researchers are looking for strategies to counteract such drawbacks, taking advantage of the characteristics of an electric propulsion system compared to a traditional one. Distributed Electric

Propulsion (DEP) is an example of this effort: thanks to electric motors scalability, the installed power can be separated into several units strategically placed to exploit positive aero-propulsive interactions.

The present thesis primarily focuses on the most common and studied DEP layout: High Lift Propellers, extending the developed methodology to Wingtip propellers whenever possible.

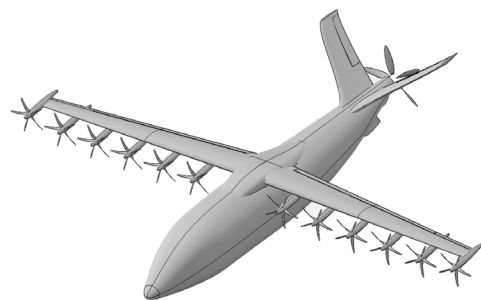


Figure 1: UNIFIER19 configuration C7A-HARW (final layout).

Figure 1 represents UNIFIER19 configuration C7A-HARW, i.e., the reference aircraft considered in this thesis; apart from the large pusher propeller on the rear of the fuselage, the airplane features 12 HLPs along the entire wingspan, including two

mounted on the wingtips. More details regarding the original C7A, from which the HARW version derives, are available in [1].

## 1.2. Objectives

The envisioned approach consists in running in advance mid-fidelity simulations of the blown layout to construct multi-dimensional maps of parameters such as lift and drag increments. The sizing routine will subsequently interrogate the dataset without a noticeable increase in the sizing loop computational costs.

To summarize, the main objectives of this thesis are:

- The **validation of a mid-fidelity method** capable of capturing the aero-propulsive interaction typical of a DEP aircraft.
- The **development of a DEP meta-model** suitable for preliminary aircraft sizing, taking advantage of the previously validated method.
- The **integration of the developed meta-model** within an existing aircraft sizing routine.

## 2. DEP modeling

Optimizations, design space explorations, and sensitivity studies, are all highly demanding tasks in terms of computational cost carried out during preliminary aircraft sizing. Procedures evaluating aerodynamics, stability, and further aspects, need to be run several times (at each iteration, for every configuration, etc.). High-fidelity models are generally too time-consuming to be integrated into sizing loops. Low- or mid-fidelity methods are thus required to complete the early design phase in a reasonable time.

The first part of the thesis surveyed some suitable methods: Vortex Lattice Method, Lifting Line Method with actuator disks, Patterson's approach [2], and DUST. The validation relied on experimental data collected by Sinnige [3] on the setup shown in Figure 2.

At first, all procedures except DUST implemented actuator disks to model the propellers, following an approach later called the AD approach. Unfortunately, the only available settings for the actuator disks were the Sinnige's measurements performed on a sting-mounted propeller that did

not include any interference effect induced on the propeller by the wing.

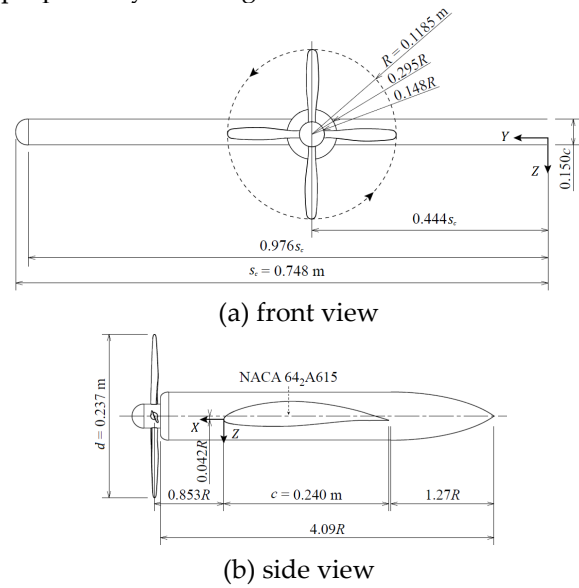


Figure 2: Sinnige's experimental setup [3].

### 2.1. Purely VLM approach

The VLM tool, just as DUST, can model the actual propeller geometry and thus capture the complete aero-propulsive coupling, paying the price of a significantly higher computational cost. The methods still implementing actuator disks can subsequently set them up relying on VLM output instead of sting-mounted propeller data. Figure 3 illustrates this approach, later called the purely VLM approach.

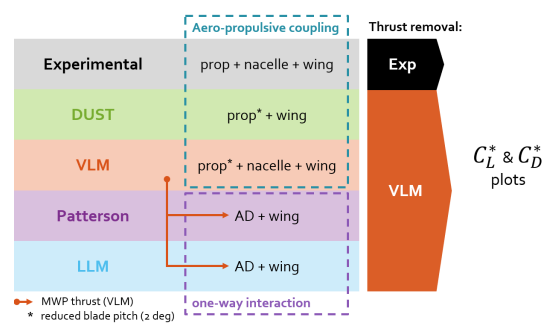


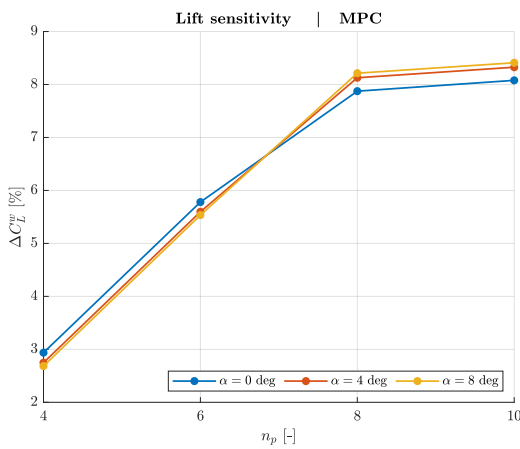
Figure 3: Purely VLM approach.

The results of a preliminary evaluation suggested abandoning both the LLM and DUST; Patterson's approach remained just as a reference since it is the method implemented in Hyperion, i.e., the preliminary sizing procedure of Politecnico di Milano. The purely VLM approach was thus the ultimate choice for the meta-model development. VSPAero, in particular, was the selected tool since

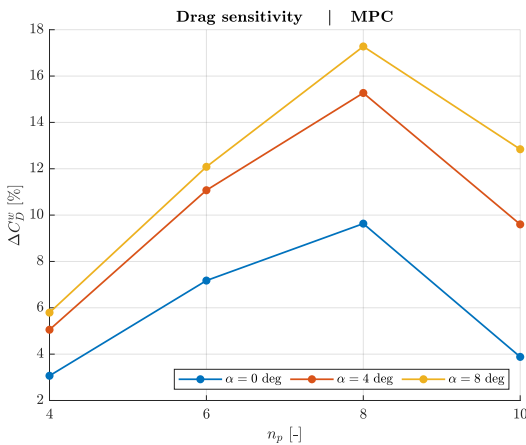
it also provides estimates of the parasite drag, but any other VLM solver may be suitable for the task if adequately validated.

## 2.2. Additional studies

Further studies analyzed the capability of the purely VLM approach to deal with setups featuring multiple, overlapping, or counter-rotating propellers. The layout used for the test is an extended version of the Sinnige's wing, shown in Figure 5; results are collected by progressively adding propellers up to five couples, starting from the innermost ones.



(a) lift coefficient increment



(b) drag coefficient increment

Figure 4: Coefficients relative increments against the number of propellers (MPC).

Figure 4 illustrates the lift and drag relative increments against the number of operative propellers with respect to the 2-prop case. Both plots exhibit an almost linear behavior up to the 8-prop case, followed by a sudden change associated with the addition of the last couple of propellers,

i.e., the WTPs. Propellers mounted on the wingtip appear to be useless in terms of lift augmentation but significant for what concerns the reduction of drag. All the propellers mounted on the same wing are co-rotating and spin in the opposite direction of wingtip vortices, i.e., inboard-up.

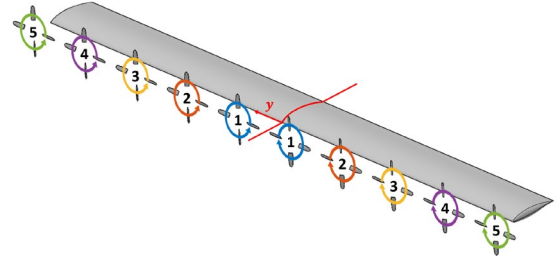


Figure 5: Multiple Propeller Case (MPC) layout.

Concerning the other studies: Propeller overlapping has almost no effects on the VLM results; the counter-rotating layout, on the other hand, is associated with a moderate drag reduction and will thus be considered for UNIFIER19.

## 2.3. Reduced approach

The high computational cost associated with MPC simulations, combined with the regularity of the lift and drag increments with the number of propellers, suggested developing a reduced approach to lower the computational costs of an extended numerical campaign while preserving the accuracy of the original simulations.

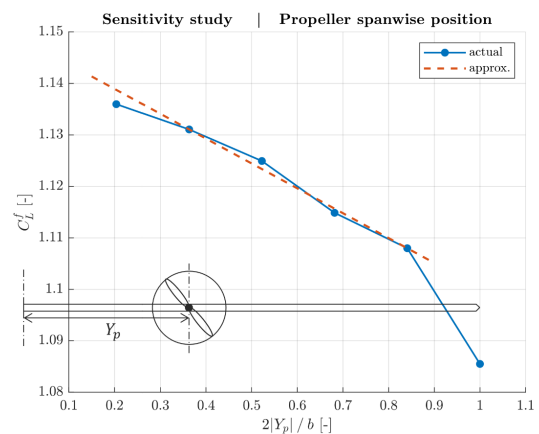


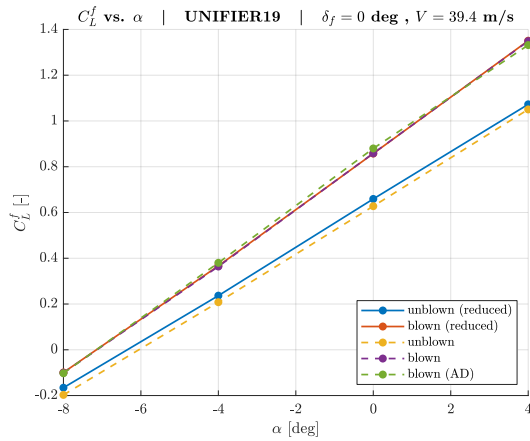
Figure 6: Lift coefficient against propeller spanwise position.

Even on a more complex geometry than the Sinnige's one, like the twisted and tapered wing of UNIFIER19, it is possible to derive an approach that allows computing the overall lift and drag

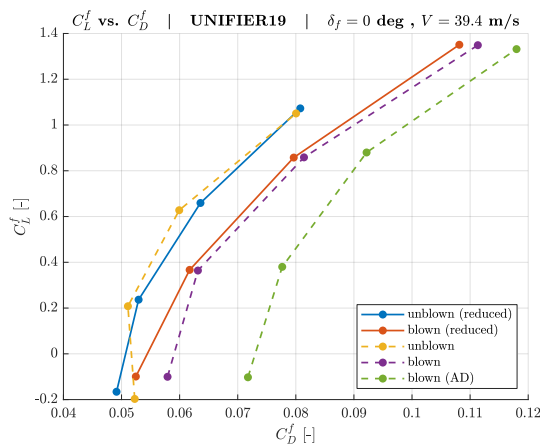
increments starting from a few low-cost simulations featuring only a limited number of propellers. Figure 6 shows the lift coefficient of a UNIFIER19 version blown by only two HLPs against the spanwise position of the propellers. The linear region on the left suggests that two simulations, each featuring a single couple of propellers, may be sufficient to compute the lift increments of all the inboard propellers. A third simulation, mounting both the couples, allows estimating the unblown wing lift coefficient. The equation to be inverted is the following:

$$\begin{bmatrix} 1 & 1 & 0 \\ 1 & 0 & 1 \\ 1 & 1 & 1 \end{bmatrix} \begin{bmatrix} C_{L_u}^f \\ \Delta C_{L_2}^f \\ \Delta C_{L_5}^f \end{bmatrix} = \begin{bmatrix} C_{L_2}^f \\ C_{L_5}^f \\ C_{L_{2\&5}}^f \end{bmatrix} \quad (1)$$

A fourth simulation featuring only the WTPs quantifies their contribution. The same approach applies to the computation of drag increments.



(a) lift polar



(b) drag polar

Figure 7: Results of the reduced approach applied to UNIFIER19.

Figure 7 compares the results of the reduced approach with those produced by the simulations of the actual completely blown UNIFIER19. The proposed method appears accurate for both the blown and the unblown curves. The estimate of the lift increment produced by the reduced approach is slightly conservative, on the other hand, the drag estimate is slightly optimistic. A correction constant with the AoA is sufficient to fix both estimates.

### 3. Meta-model development

Implementing the presented methodology in a preliminary sizing tool requires an extensive numerical campaign to construct a suitable dataset that TITAN procedures will interrogate during the sizing loop.

#### 3.1. Dimensional analysis

The dimensional analysis of a generic force coefficient provided a consistent framework for the design of the numerical campaign and the construction of the meta-model dataset. The expression of a generic aero-propulsive force acting on a blown wing is the following:

$$F = F(\rho, a, \mu, V, \alpha, S, \epsilon, d, N) \quad (2)$$

where the force  $F$  is assumed to depend on the air density  $\rho$ , the speed of sound  $a$ , the air viscosity  $\mu$ , the airspeed  $V$ , the angle of attack  $\alpha$ , the wing surface  $S$ , the propeller tilt angle with respect to the wing reference chord  $\epsilon$ , the propeller diameter  $d$ , and the propeller RPM  $N$ . According to the Buckingham  $\pi$  theorem, given the presence of eight dimensional quantities and three physical dimensions, it is possible to rewrite Eq. (2) as a function of five dimensionless groups:

$$\pi_1 = \frac{F}{\rho V^2 S} = \frac{C_F}{2} \quad (3)$$

$$\pi_2 = \frac{V}{a} = M \quad (4)$$

$$\pi_3 = \frac{\rho V \sqrt{S}}{\mu} \sim \text{Re} \quad (5)$$

$$\pi_4 = \frac{d}{\sqrt{S}} = r_p \quad (6)$$

$$\pi_5 = \frac{V}{N \sqrt{S}} = J r_p \quad (7)$$

The dimensionless form of Eq. ( 2 ) is finally the following:

$$C_F = C_F(M, Re, r_p, J, \alpha, \epsilon) \quad (8)$$

where the force coefficient  $C_F$  is a function of the Mach number  $M$ , the Reynolds number  $Re$ , the geometrical parameter  $r_p$ , the advance ratio  $J$ , and the two already dimensionless quantities  $\alpha$  and  $\epsilon$ .

### 3.2. Numerical campaign

The selection of UNIFIER19 configuration C7A-HARW as the reference geometry for the numerical campaign reduces the design space to three parameters: the AoA, the propeller tilt, and the advance ratio. A typical low-speed and low-altitude scenario fixes both the Mach and Reynolds numbers. Regarding the geometrical parameter  $r_p$ , its value does not change throughout the design loop since the Hyperion input file sets both the number of HLPs and the wing aspect ratio.

Case ID	$\epsilon$	$J$
MM.tm12.J08	$-12^\circ$	0.8
MM.tm12.J12	$-12^\circ$	1.2
MM.tm12.J16	$-12^\circ$	1.6
MM.tm6.J08	$-6^\circ$	0.8
MM.tm6.J12	$-6^\circ$	1.2
MM.tm6.J16	$-6^\circ$	1.6
MM.t0.J08	$0^\circ$	0.8
MM.t0.J12	$0^\circ$	1.2
MM.t0.J16	$0^\circ$	1.6

Table 1: List of numerical campaign cases.

Table 1 lists the nine cases considered for the numerical campaign, they correspond to all the possible combinations of the three selected values of propeller tilt and advance ratio. Both reference [1] and UNIFIER19 OpenVSP model provided meaningful information to assume two plausible ranges.

Figure 8 illustrates the four layouts used to apply the reduced approach to UNIFIER19; this approach proved its effectiveness in lowering the computational costs of the numerical campaign by about 50% without compromising the accuracy.

The dataset, made of 216 data points divided into 36 raw data curves, generates nine sets of polars, corresponding to the nine cases of Table 1,

representing the multi-dimensional maps of increments and coefficients.

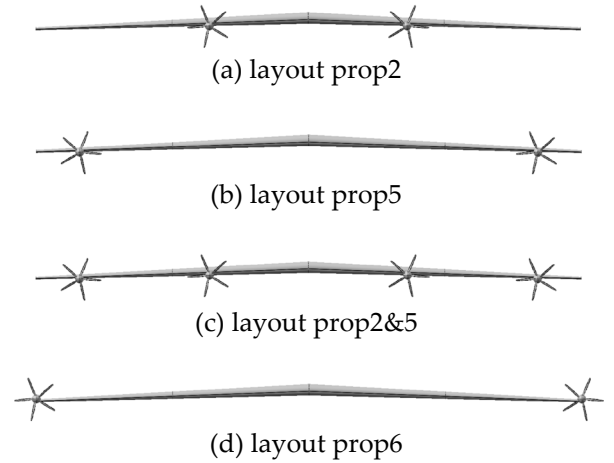


Figure 8: Geometrical setups used in the numerical campaign to apply the reduced approach.

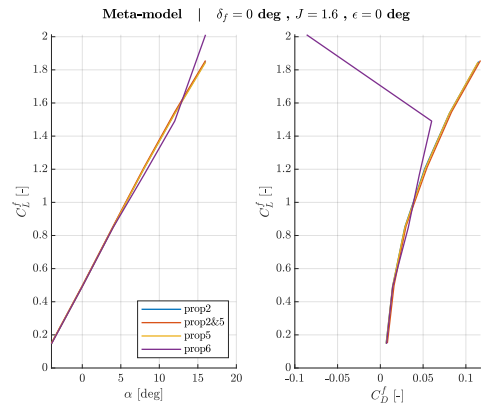


Figure 9: Example of a poorly converged polar (raw data).

Figure 9 shows one of the few curves containing some corrupted data points; their correction, which requires human judgment, is left entirely manual.

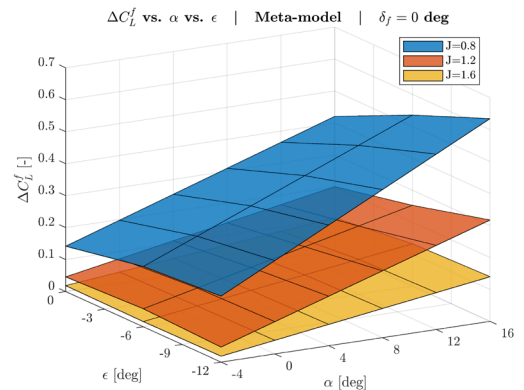


Figure 10: Lift coefficient increment multi-dimensional map.

Figure 10 shows an example of the multi-dimensional maps of the coefficients increments obtained thanks to the numerical campaign.

### 3.3. Proposed architecture

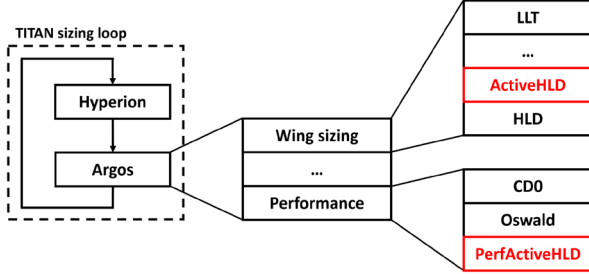


Figure 11: Proposed Argos architecture.

The main additions to the current architecture of Argos are the two functions highlighted in red in Figure 11:

- The **ActiveHLD** module computes the propeller operative settings, i.e., their RPM, to obtain the desired lift augmentation estimated by Patterson's method in Hyperion.
- The **PerfActiveHLD** module, given the HLP settings determined by ActiveHLD, updates the parabolic polars generated by the existing methods adding the contributions of the DEP system.

Preprocessing tools, able to deal even with future and more extended numerical campaigns, were also developed.

## 4. Results

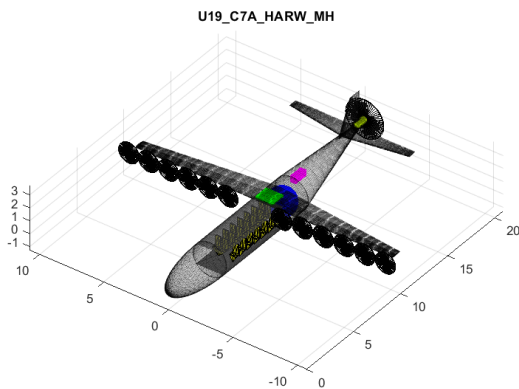


Figure 12: UNIFIER19 configuration C7A-HARW (TITAN solution).

Firstly, TITAN had to size configuration C7A-HARW without the meta-model; this represents the reference solution for all the following comparisons. Figure 12 depicts the geometry generated by TITAN. Apart from the different layout of the empennage, only some minor discrepancies are present between the OpenVSP model provided by PVS, representing the final layout of UNIFIER19, and the TITAN solution, which is the mere result of an automatic sizing procedure.

Table 2 shows the minimum propeller RPM required to obtain the desired lift increment in some significant flight conditions. The method also estimates the DEP throttle parameter and the power repartition between DEP and the main motor. This result is not an actual propeller scheduling, which requires enforcing many more constraints but provides a bunch of meaningful information to assess the solidity of the solution.

	$N$	$\sigma_{DEP}$	$P_{\%}^{DEP}$
@ stall (clean)	1285 RPM	28%	30%
@ TO speed	1299 RPM	37%	39%
@ LND speed	1315 RPM	41%	37%
@ stall (TO)	1390 RPM	51%	60%
@ stall (LND)	1573 RPM	86%	95%

Table 2: HLP settings to obtain the desired lift increments in some flight conditions.

Concerning the drag polars, the procedure corrects the Oswald factor of the takeoff and landing configurations, previously left unchanged; it also corrects the minimum drag coefficient, which currently does not considers the contribution of the HLPs nacelles.

	Current [kg]	Proposed [kg]	Variation [%]
Structure + Systems	4086.7	4136.1	+1.2
Crew + Payload	2380.0	2380.0	0.0
LH2 related	938.4	1069.3	+13.9
Battery	681.7	641.3	-5.9
<b>MTOM</b>	<b>8086.8</b>	<b>8226.7</b>	<b>+1.7</b>

Table 3: Mass increment breakdown.

The MTOM of UNIFIER19 increased by 1.7% due to the new changes. Table 3 presents the breakdown of the mass increments introduced by applying the meta-model. All the items considered by TITAN fall in one of the four categories shown in the table, which separate the components according to the magnitude of their mass relative increment. The higher drag directly impacts the energy consumption and thus all the LH2-related elements, i.e., fuel, fuel tank, and PGS. The battery, on the other hand, benefits from the more powerful PGS and its mass thus decreases.

## 5. Conclusion

The developed meta-model is successfully implemented in TITAN, the preliminary aircraft sizing routine of Politecnico di Milano.

The results confirm that the ranges selected for the meta-model parameters are adequate, neither too narrow nor too broad; they cover all the design space without, at the same time, wasting resources in the construction of a pointlessly large map.

The HLP settings provide some meaningful information for a more detailed sizing of the DEP system; the DEP throttle parameter confirms that the installed DEP power is sufficient for every flight condition. The power repartition, every time below 100%, ensures that the DEP power needed to augment the lift never exceeds the required power. Therefore, the DEP system alone will never produce a positive excess power, which is highly undesirable in phases such as landing.

Finally, the MTOM increment highlighted a possibly significant deficiency of the current version of TITAN concerning drag estimation; the procedure, which entirely relied on Patterson's approach to estimate the DEP effects, neglected the contribution of the several added nacelles.

### 5.1. Future developments

The ideas implemented in this thesis are relatively few, considering the potential offered by the meta-model concept in general.

The most significant envisioned proposal concerns some additional features for TITAN, unluckily not developed due to the lack of time to run the new numerical campaign. These features include a method to deal consistently with the overall lift increment, jointly produced by flap and DEP.

The further proposals concern an automatic procedure to speed up the setup of the VSPAero simulations, a function to compute the actual motor scheduling, VLM-derived multi-dimensional maps for the unblown layout, etc.

## References

- [1] UNIFIER19, "D2.2: Final concurrent design report," 2021. [Online]. Available: [https://www.unifier19.eu/wp-content/uploads/2021/07/D2.2\\_Final\\_concurrent\\_design\\_report\\_Open.pdf](https://www.unifier19.eu/wp-content/uploads/2021/07/D2.2_Final_concurrent_design_report_Open.pdf).
- [2] M. D. Patterson, "Conceptual design of high-lift propeller systems for small electric aircraft," PhD Thesis. Georgia Institute of Technology, 2016.
- [3] T. Sinnige, N. van Arnhem, T. C. A. Stokkermans, E. Georg and L. L. M. Veldhuis, "Wingtip-Mounted Propellers: Aerodynamic Analysis of Interaction Effects and Comparison with Conventional Layout," *Journal of Aircraft*, pp. 295-312, 2019.

## 6. Acknowledgments

Firstly, I would like to express my gratitude to my thesis supervisor and his team, Professor Lorenzo Trainelli, Professor Carlo E. D. Riboldi, and Yasir Khan, for their support throughout this work.

Thank you also to my colleagues, my friends, and my relatives. A special thanks to my parents, Morena and Gabriele, for the tireless and unconditional sustain they provided me over the last almost 25 years.